MECHANOCHEMICAL PREPARATION OF $BaTiO_3$-Ni NANOCOMPOSITES WITH HIGH DIELECTRIC CONSTANT

PEDRO E. SÁNCHEZ-JIMÉNEZ, LUIS A. PÉREZ-MAQUEDA*, MARÍA J. DIÁNEZ, ANTONIO PEREJÓN AND JOSÉ M. CRIADO

Instituto de Ciencia de Materiales de Sevilla

C.S.I.C. - Universidad de Sevilla

C. Américo Vespucio 49, 41092 Sevilla, Spain

Abstract

A mechanochemical procedure is proposed for an easy preparation of a $BaTiO_3$-Ni composite in a single steep. $BaTiO_3$ and Ni powders available in the market are mixed by dry ball milling producing a decrease of particle size and an evenly distribution of both phases. In the sintered pellets the nickel particles are homogeneously distributed into the $BaTiO_3$ matrix and isolated from others Ni particles. The dielectric constant of the composite is considerably higher than that of the barium titanate. Moreover, the temperature of the ferroelectric ↔ paraelectric transition of the $BaTiO_3$-Ni composite here prepared is much lower than the one of the pure $BaTiO_3$ single phase.

- Corresponding author, e-mail: maqueda@cica.es

Introduction

Ferroelectric ceramics are widely used in a broad range of applications, especially in the design of electronic devices such as capacitors, dielectrics or electroactive materials [1-3]. Barium titanate ($BaTiO_3$) is one of the most used ferroelectric ceramic in electronics due to its high dielectric constant, which makes it a very attractive material to use in capacitors such as boundary layer capacitors (BLC) and multilayer ceramic capacitors (MLCC) [3-5]. Because of its extensive use, it has been widely studied and several methods have been proposed to enhance its dielectric constant. Thus, it has been observed that the homogeneous dispersion of an electrically conductive filler, such as small metal particles, into an insulating matrix leads to an increase in the dielectric constant of the composite [3, 6]. This raise reaches its maximum in the neighbourhood of the percolation threshold, where the dielectric constant experiments an abrupt increase [7-9]. As the metal content grows over the percolation threshold, an insulator-conductor transition is recorded and both conductivity and permittivity increase [10, 11]. This phenomenon may be explained by the isolation of the metal particles by thin dielectric layers near the percolation threshold. Hence the composite turns into a capacitor with good charge storage properties. This behaviour is well known and it has been explained by the percolation theory [12]. Moreover, it has been observed that the incorporation of metal particles improve the sintering process, because metal particles undergo plastic deformation and thereby relax the internal stresses induced during the sintering [3, 13-17].

These kind of insulator/conductor composites have been intensely investigated in the last years [3, 18-21] and present a great scientific and engineering interest. Recently, Pecharroman *et al* [22] have designed a $BaTiO_3$-Ni composite with an extremely high dielectric constant. In a similar way, Chen *et al* [3] reported the enhancement of the dielectric properties of X7R barium titanate ceramic by addition of nickel nanoparticles, while Qiao and Bi observed an improvement in the dielectric behaviour of $BaTiO_3$-Ni composite ferroic film. Lin *et al* [23] registered an analogue behaviour when incorporating silver particles to an NBT ceramic matrix, Panteny *et al* in barium titanate-silver composite [11] and George *et al* in barium samarium titanate-silver composite [10].

The most common method of preparing these metal-ceramic composites is colloidal processing, which implies using nanoparticles of both constituents and high volumes of water [7, 22]. Other methods involves using co-sputtering methods[24] or wet grinding [10]. In this work we propose the preparation $BaTiO_3$-Ni nanocomposites by dry grinding stating form conventional powders. Additionally, the dielectric behaviour of $BaTiO_3$-Ni nanocomposite prepared are investigated.

Experimental

The composites were prepared from commercial Ni (Sigma-Aldrich 266981-500G, 3µm, 99.7 % in purity) and $BaTiO_3$ (Aldrich 12047-27-7, 2µm, 99.9 % in purity) samples. Powder mixtures containing 28 vol % nickel and 72 vol % $BaTiO_3$ were placed in a agate jar (300 cc volumen) with 12 agate balls 20 mm in diameter and milled using a centrifuge mill (model Fritsch Pulverisette) at 730 r.p.m. Different milling times were used for comparison. The surface areas of all powders were determined with a surface area analyzer (model FlowSorb III 2310, Micrometrics Instruments), using N_2 as an adsorbate at the liquid nitrogen temperature. Size measurements were also made by light scattering procedure by means of a particle size analyzer (model Matersizer, Malvern)

Ball milled powders were pressed into discs of 13 mm in diameter and 1 mm in thickness by uniaxial pressing at 860 MPa. Then, the discs were sinterized at 1300ºC under N_2 atmosphere for 2 hours using a Carbolite 1500ºC horizontal tube furnace. The densities of all discs were determined both before and after sintering using the Archimedes method.

Dilatometric curves for pure $BaTiO_3$ and for $BaTiO_3$-Ni composite under nitrogen atmosphere were obtained with a home-made dilatometer that measures the thickness change with temperature during the sintering process.

The microstructures of both powders and sintered discs were studied by scanning electron microscopy (SEM)) in a Jeol instrument equipped with energy dispersive x-ray spectrometer (EDX).

X-ray powder diffraction patterns were obtained with a Siemens D501 instrument using CuK_{α} radiation and a graphite monochromator. The full-width of the half-maximum (FWHM) of (111) diffraction peak was used for calculating the coherently diffracting domain for both Nickel and $BaTiO_3$ particles, according to the Scherrer equation.

The sintered discs were placed between two platinum electrodes for measuring their dielectric constant and the dielectriuc loss by means of a LCR meter (IET, model IMF 600A). The two parallel surfaces of the sintered discs where covered with gold by means of a sputtering device for improving the electrical contact with the platinum electrodes.. The temperature dependences of the dielectric constant and dielectric loss were measured at temperatures ranging from 25ºC to 200ºC at 1 KHz.

Results and discussion

Fig. 1 shows the XRD patterns corresponding to a starting barium titanate and nickel mixture before milling (Fig. 1a) and to a $BaTiO_3$-Ni powder milled for one (Fig. 1b), four (Fig. 1c) and eight hours (Fig. 1d). Both phases, Ni and $BaTiO_3$, remain crystalline after grinding treatment, but diffraction peaks becomes broader with the treatment due to a decrease in crystallite size. Thus, the crystallite size decreases for the starting powders from 117.0 and 136.3 nm for the $BaTiO_3$ and Ni, respectively, to about 45.5 and 63.8 nm for the $BaTiO_3$ and Ni, respectively, after grinding for one hour (Table 1). As grinding time proceeds, crystalline sizes decrease, yielding a minimum value of 28.4 and 30.3 nm for the $BaTiO_3$ and Ni, respectively, after eight hours treatment. The BET specific surface values obtained for the different milled samples are presented in Fig. 2. The specific surface value quickly rises with the grinding time, from about 1.2 m^2 g^{-1} for the unmilled sample to a maximum value of 11.6 m^2 g^{-1} for the sample ground for four hours. After 4 hours of milling, the specific surface start to decrease until reaching a stade state value of 7.4 m^2 g^{-1} from 8 hours of treatment. Thus, these results indicate that although the crystallite size decreases with the grinding time in entire studied range, surface area reaches a maximum at a 4-hour of milling time, and starts decreasing thereafter, probably due to aggregation produced by the grinding procedure.

Fig. 3 shows the scanning electron micrographs of starting nickel and barium titanate powders (Figs. 1a and 1b, respectively) and $BaTiO_3$-Ni powder milled for 4 hours (Fig. 1c). Original powders consist of irregular and micron-sized particles highly aggregated. It can be appreciated that composite particles are also highly aggregated, although the subunits are smaller than in the starting powders. The micrograph of milled sample also reveals that nickel and $BaTiO_3$ particles presents a very homogeneous distribution, which is proved by the EDX mapping made for further confirmation, and presented in Fig. 1d.

Fig. 4 shows the particle size distribution curves as obtained by light scattering procedure for the starting powders and the composite. As shown in the figure, both $BaTiO_3$ and Ni starting powders have a broad particle size distribution with modal sizes at 2.65 µm and 7.35 µm for $BaTiO_3$ and Ni, repectively. For the mixture ball-milled for four hours, the modal size decreases to 1.41 µm, but the curve shows a very broad particle size distribution because of the high degree of aggregation of the small particles, as also observed in the SEM micrograph (Fig. 3. c).

Fig. 5 shows the dilatometric curves obtained for both pure $BaTiO_3$ and $BaTiO_3$-Ni sample milled for four hours. Both dilatometric curves are quite similar except for a slight shift to lower temperatures for the $BaTiO_3$-Ni composite due to the inclusion of metal particles in the barium titanate matrix, which promotes the sintering process. This behaviour could be understood in terms of a plastic deformation of the metallic particles that relax the internal stresses that occurs during the sintering [3, 13-17]. The dilatometric curve shows that sintering is complete at 1300ºC, therefore, composite pellets were prepared from the $BaTiO_3$-Ni powder milled during 4 hours by sintering the pressed powders at 1300ºC under N_2 atmosphere for 2 hours. The density of the pellets thus obtained was measured by the Archimedes method, yielding a final densification of 98%. In Fig. 6 a scanning electron micrograph taken from the surface of the sintered sample is presented, as well as a Ni and Ti mapping image, showing an evenly dispersion of nickel particles into the $BaTiO_3$ matrix. Thus, nickel particles are surrounded by the $BaTiO_3$ phase and isolated from other Ni particles, indicating that the system has not overpassed the percolation threshold.

Fig. 7 shows the dependence of the dielectric constant and the dielectric loss of the composites on the temperature. It is noteworthy the significant effect the inclusion of metal particles have on the dielectric behaviour of the $BaTiO_3$. The dielectric constant of the $BaTiO_3$-Ni is much higher than that of the pure $BaTiO_3$ in the entire range of temperature studied, while the maximum values for both pure $BaTiO_3$ and $BaTiO_3$-Ni are 470 and 10850, respectively. Additionally, the maximum of the dielectric constant that occurs at 122-125ºC [25-30] in $BaTiO_3$ and is associatecd to a ferroelectric (tetragonal) to paraelectric (cubic) phase transition is moved down to 82ºC in the $BaTiO_3$-Ni nanocomposite. Moreover, the very low dielectric loss of this composite (about 0.04) supports the high quality of the dielectric here prepared.

Conclusions

An easy and rapid method for obtaining $BaTiO_3$-Ni nanocomposites by mechanical grinding has been developed. This method allows working with conventional starting powders, because the milling itself reduces particle size at the same time that the components get thoroughly dispersed, thus obtaining a homogeneous nanocomposite by a simple procedure in a single step. The incorporation of metal nickel particles into a barium titanate matrix results in an improvement of the electric properties over the pure ferroelectric matrix. The high dielectric constant presented by the nanocomposite and the simple preparation procedure makes it an attractive material for different technological applications.

References

[1] Haertling GH. Ferroelectric ceramics: History and technology. Journal Of The American Ceramic Society 1999;82:797-818.

[2] Chen FT, Chu CW, He J, Yang Y, Lin JL. Organic thin-film transistors with nanocomposite dielectric gate insulator. Applied Physics Letters 2004;85:3295-7.

[3] Chen RZ, Wang XH, Wen H, Li LT, Gui ZL. Enhancement of dielectric properties by additions of Ni nano-particles to a X7R-type barium titanate ceramic matrix. Ceramics International 2004;30:1271-4.

[4] Guillemet-Fritsch S, Valdez-Nava Z, Tenailleau C, Lebey T, Durand B, Chane-Ching JY. Colossal permittivity in ultrafine grain size BaTiO3-x and Ba0.95La0.05TiO3-x materials. Advanced Materials 2008;20:551-+.

[5] Hsi CS, Chen YC, Jantunen H, Wu MJ, Lin TC. Barium titanate based dielectric sintered with a two-stage process. Journal of the European Ceramic Society 2008;28:2581-8.

[6] Grannan DM, Garland JC, Tanner DB. Critical-Behavior of the Dielectric-Constant of a Random Composite near the Percolation-Threshold. Physical Review Letters 1981;46:375-8.

[7] Pecharroman C, Moya JS. Experimental evidence of a giant capacitance in insulator-conductor composites at the percolation threshold. Advanced Materials 2000;12:294-7.

[8] Dang ZM, Fan LZ, Shen Y, Nan CW. Study on dielectric behavior of a three-phase CF/(PVDF+BaTiO3) composite. Chemical Physics Letters 2003;369:95-100.

[9] Meir Y. Percolation-type description of the metal-insulator transition in two dimensions. Physica a-Statistical Mechanics and Its Applications 2001;302:391-403.

[10] George S, Santha NI, Sebastian MT. Percolation phenomenon in barium samarium titanate-silver composite. Journal of Physics and Chemistry of Solids 2009;70:107-11.

[11] Panteny S, Bowen CR, Stevens R. Characterisation of barium titanate-silver composites part II: Electrical properties. Journal of Materials Science 2006;41:3845-51.

[12] Nan CW. PHYSICS OF INHOMOGENEOUS INORGANIC MATERIALS. Progress in Materials Science 1993;37:1-116.

[13] Chen CY, Tuan WH. Effect of silver on the sintering and grain-growth behavior of barium titanate. Journal of the American Ceramic Society 2000;83:2988-92.

[14] Hwang HJ, Yasouka M, Sando M, Toriyama M, Niihara K. Fabrication, sinterability, and mechanical properties of lead zirconate titanate/silver composites. Journal of the American Ceramic Society 1999;82:2417-22.

[15] Pearce DH, Button TW. Processing and properties of silver/PZT composites. Ferroelectrics 1999;228:91-8.

[16] Zhang HL, Li JF, Zhang BL. Sintering and piezoelectric properties of Co-fired lead zirconate titanate/Ag composites. Journal of the American Ceramic Society 2006;88:1300-7.

[17] Zhang HL, Li JF, Zhang BL, Jiang W. Enhanced mechanical properties in Ag-particle dispersed PZT piezoelectric composites for actuator applications. Materials Science and Engineering: A 2008;498:272-7.

[18] Dang ZM, Fan LZ, Shen Y, Nan CW. Dielectric behavior of novel three-phase MWNTs/BaTiO3/PVDF composites. Materials Science and Engineering B-Solid State Materials for Advanced Technology 2003;103:140-4.

[19] Bai Y, Cheng ZY, Bharti V, Xu HS, Zhang QM. High-dielectric-constant ceramic-powder polymer composites. Applied Physics Letters 2000;76:3804-6.

[20] Dang ZM, Shen Y, Nan CW. Dielectric behavior of three-phase percolative Ni-BaTiO3/polyvinylidene fluoride composites. Applied Physics Letters 2002;81:4814-6.

[21] Duan N, ten Elshof JE, Verweij H, Greuel G, Dannapple O. Enhancement of dielectric and ferroelectric properties by addition of Pt particles to a lead zirconate titanate matrix. Applied Physics Letters 2000;77:3263-5.

[22] Pecharroman C, Esteban-Betegon F, Bartolome JF, Lopez-Esteban S, Moya JS. New percolative BaTiO3-Ni composites with a high and frequency-independent dielectric constant (epsilon(r) approximate to 80,000). Advanced Materials 2001;13:1541-+.

[23] Lin YH, Nan CW, Wang JF, Liu G, Wu JB, Cai N. Dielectric behavior of Na0.5Bi0.5TiO3-based composites incorporating silver particles. Journal of the American Ceramic Society 2004;87:742-5.

[24] Qiao L, Bi XF. Dielectric behavior of BaTiO3-Ni composite ferroic films. Applied Physics a-Materials Science & Processing 2009;95:733-8.

[25] Delcerro J, Mundi M, Gallardo C, Criado JM, Gotor FJ, Bhalla A. Sintering temperature influence on phase-stability of barium titanat ceramics with very small grain size. Ferroelectrics 1992;127:59-64.

[26] van der Gijp S, Winnubst L, Verweij H. Peroxo-oxalate preparation of doped barium titanate. Journal of the American Ceramic Society 1999;82:1175-80.

[27] Alcala MD, Criado JM, Dianez MJ, Gotor FJ, Perez-Maqueda LA, Real C. Development of an experimental tool for measuring electrical properties of materials from liquid nitrogen temperature up to 1000 degrees C. Thermochimica Acta 2000;351:125-30.

[28] Perez-Maqueda LA, Dianez MJ, Gotor FJ, Sayagues MJ, Real C, Criado JM. Synthesis of needle-like BaTiO3 particles from the thermal decomposition of a citrate

precursor under sample controlled reaction temperature conditions. Journal of Materials Chemistry 2003;13:2234-41.

[29] Smith MB, Page K, Siegrist T, Redmond PL, Walter EC, Seshadri R, et al. Crystal structure and the paraelectric-to-ferroelectric phase transition of nanoscale BaTiO3. Journal of the American Chemical Society 2008;130:6955-63.

[30] Sedykh P, Haase J, Michel D, Charnaya EV. Investigation of barium titanate nanoparticles by Ba-137 NMR. Ferroelectrics 2008;363:215-26.

Table 1.

Coherently Diffracting Domains values corresponding to starting nickel and barium titanate powders, and to the nanocomposite after different milling times.

Sample	Milling Time (hour)	d_{111} (nm) $BaTiO_3$	d_{111} (nm) Ni
Starting $BaTiO_3$	0	117.0	-
Starting Nickel	0	-	136.3
$BaTiO_3$-Ni mixture	1 2 4 8	45.5 38.8 37.5 28.4	63.8 58.7 49.4 30.3

Figure captions

Fig 1. X-ray diffraction patterns of barium titanate and nickel mixture before milling (a) and after grinding for one (b), four (c), and eight (d) hours. Peaks corresponding to Ni phase are marked with an asterisk, all other peaks correspond to $BaTiO_3$ phase.

Fig 2. BET specific surface values for the $BaTiO_3$-Ni composite powder after different milling times.

Fig 3. Scanning electron microscopy micrographs illustrating the morphology of (a) Nickel and (b) $BaTiO_3$ starting powders; (c) $BaTiO_3$-Ni powder milled during 4 hours; (d) Ni element mapping that correspond to the field of vision in (c).

Fig 4. Particle size distribution for (a) $BaTiO_3$ and (b) Nickel starting powders, and (c) BaTiO3-Ni powder milled for 4 hour.

Fig 5. Dilatometric curves corresponding to: (a) pure $BaTiO_3$ milled for 4 hours and (b) $BaTiO_3$-Ni powders 4 hours milled.

Fig 6. Scanning electron microscopy micrograph (a) showing the microstructure of sintered $BaTiO_3$-Ni bodies. (b) Ni and (c) Ti element mapping that correspond to the field of vision in (a).

Fig 7. (a) Values for dielectric constant ε for both pure BaTiO3 and the $BaTiO_3$-Ni nanocomposite and (b) dielectric loss of the $BaTiO_3$-Ni composite as a function of temperature.

Figure
Click here to download high resolution image

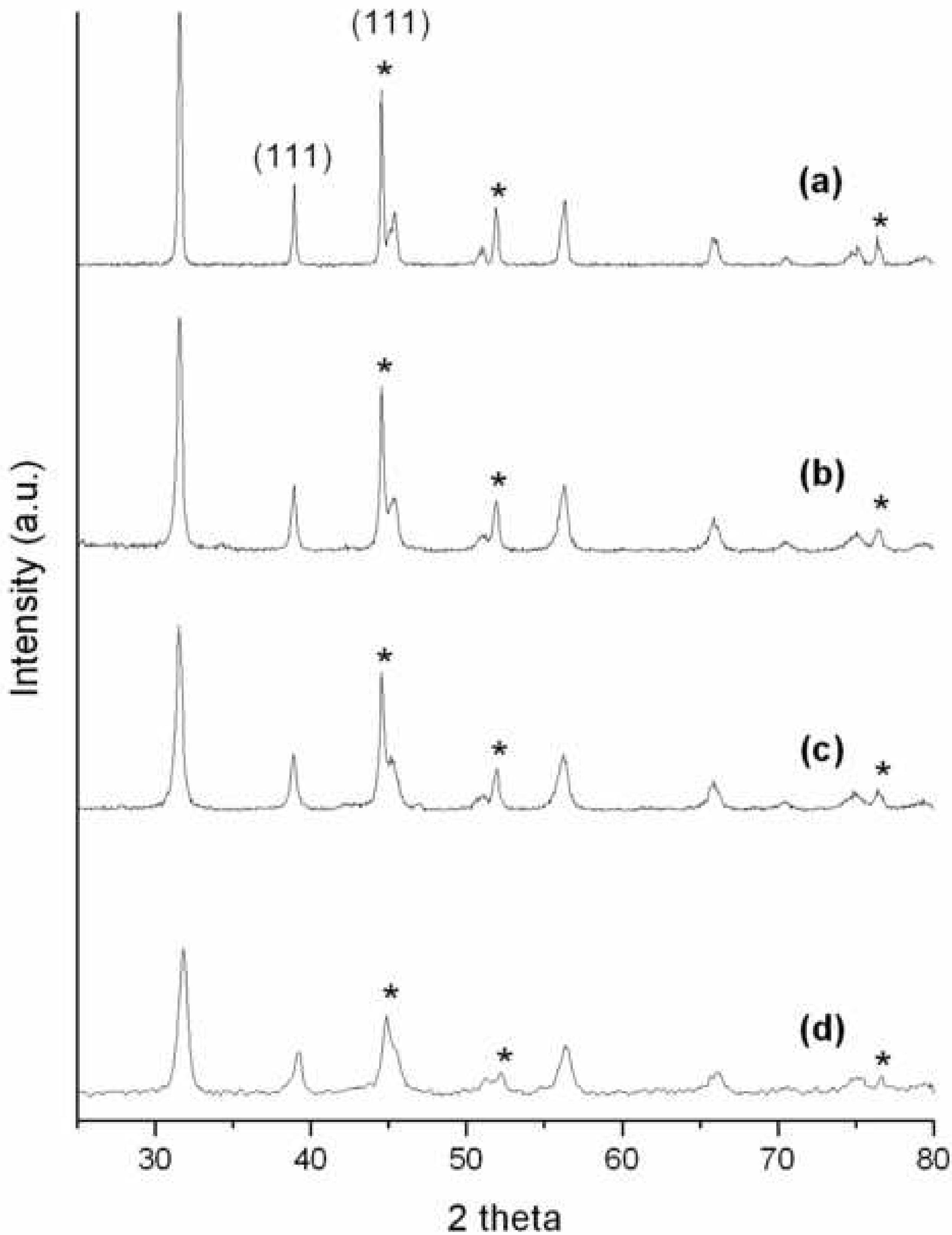

Figure
Click here to download high resolution image

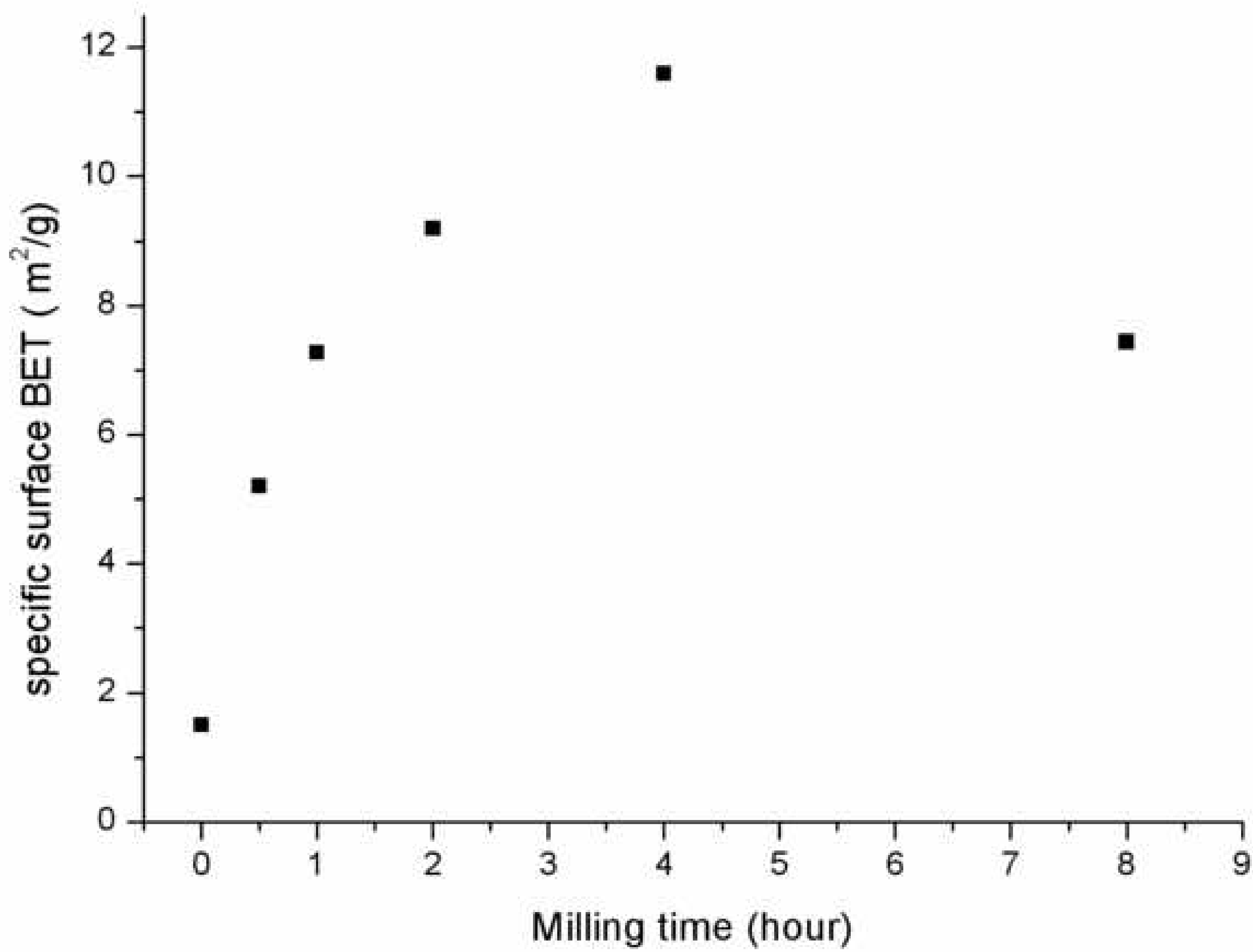

Figure
Click here to download high resolution image

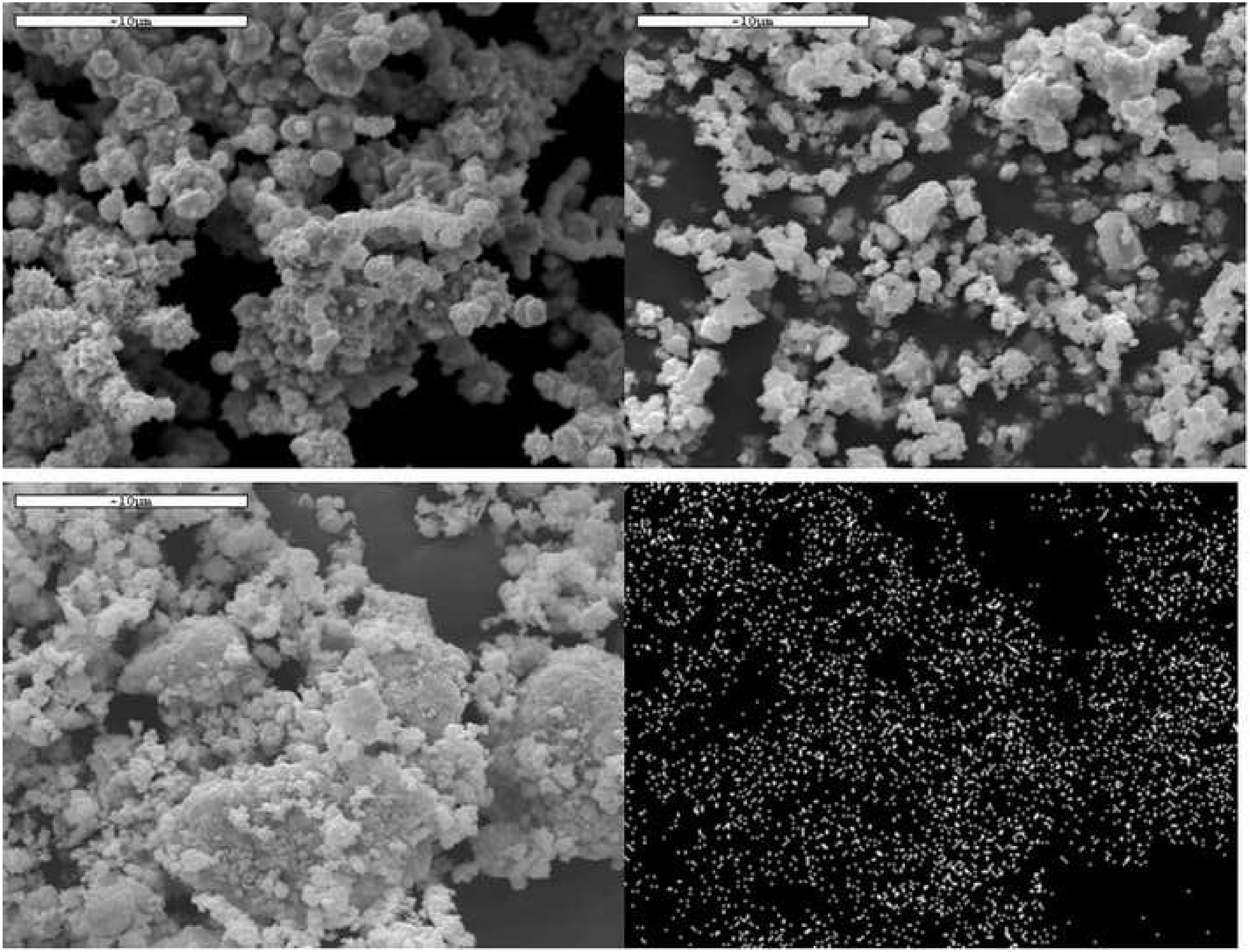

Figure
Click here to download high resolution image

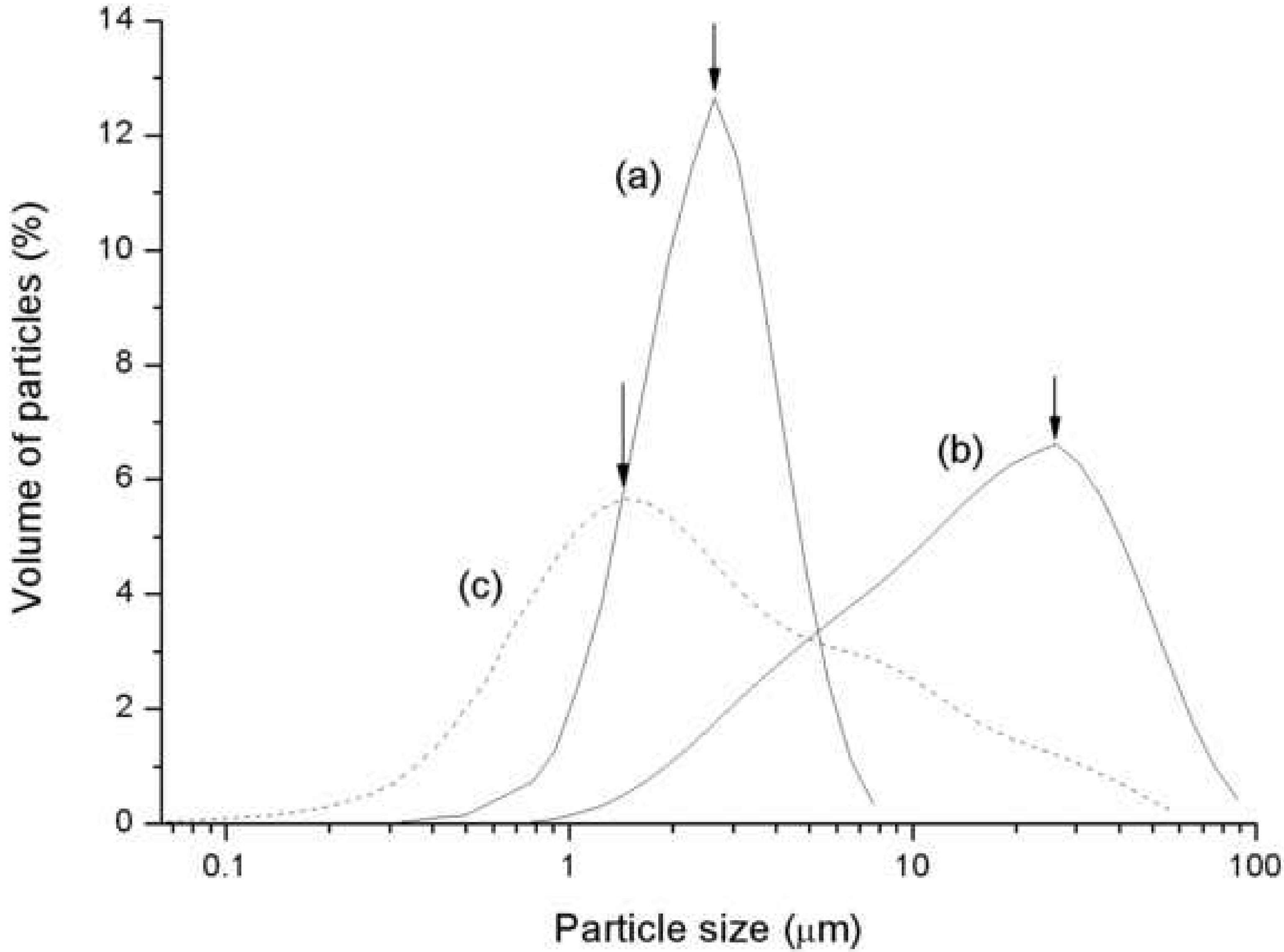

Figure
Click here to download high resolution image

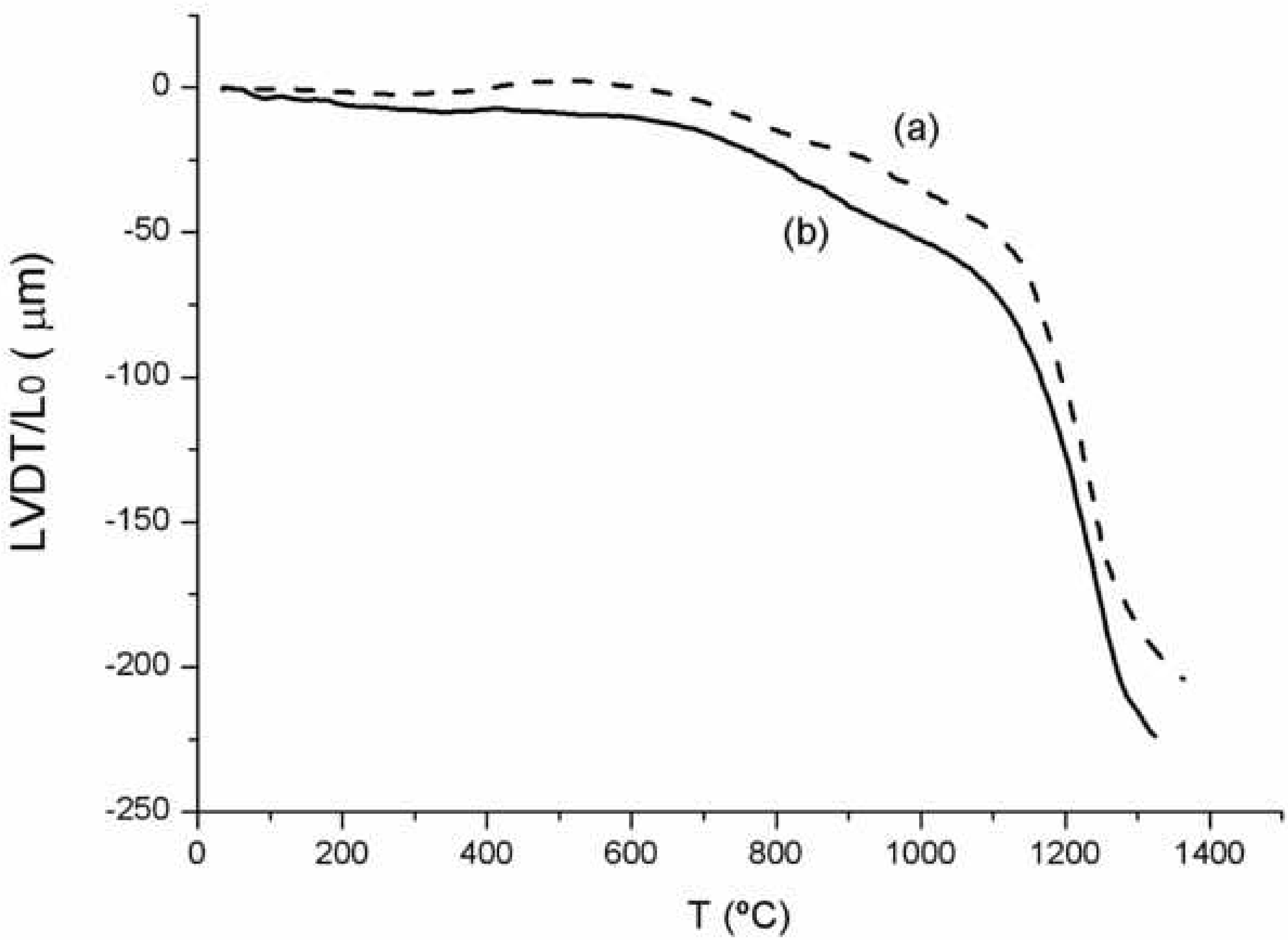

Figure
Click here to download high resolution image

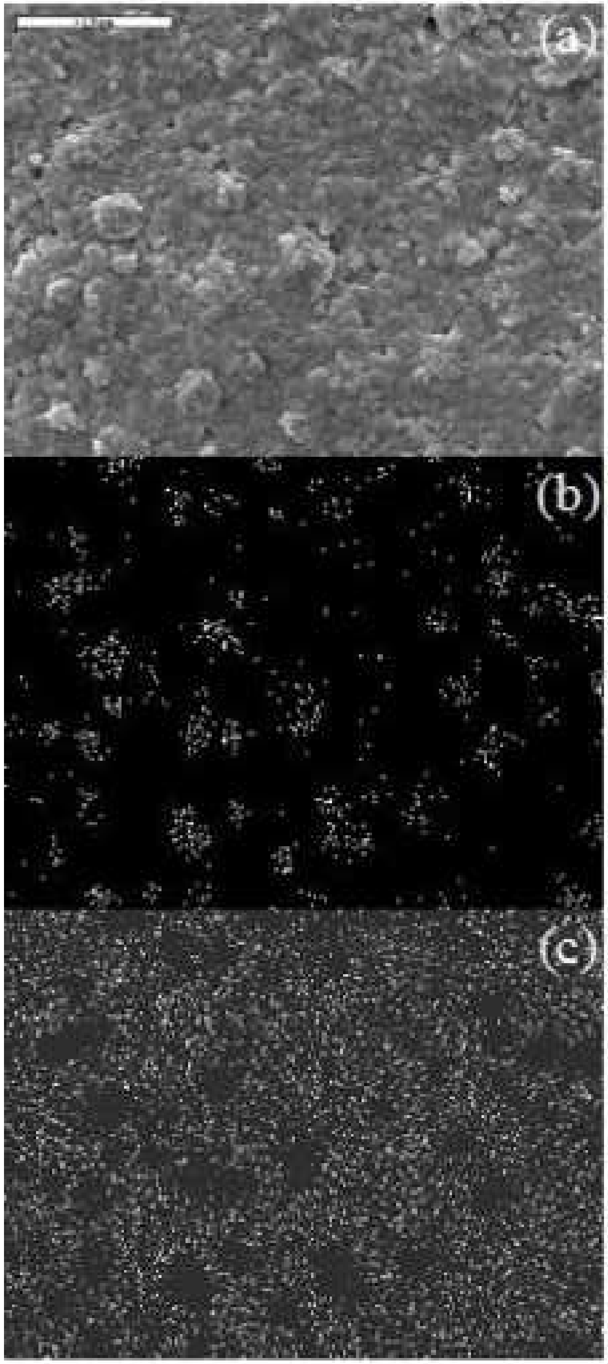

Figure
Click here to download high resolution image